Improving Fat Saturation in MRI of the Cervical Spine and Foot at 1.5T Using Patient-Specific Spectral-Spatial Radiofrequency Pulses

Jonathan van Dieken, M.D.; Simon F. Rösel, M.D.; Ali Seif Amir Hosseini, M.D.; Babak Panahi, M.D.; Guenther Engel, M.D.

Department of Clinical and Interventional Radiology, University Medical Center Göttingen, Germany

Abstract

Background
Conventional chemical shift-selective fat saturation ($CHESS_{standard}$) frequently fails in the presence of susceptibility-induced static magnetic field inhomogeneities. Patient-specific spectral-spatial radiofrequency pulses ($CHESS_{SPSP}$) promise enhanced fat saturation in challenging body regions such as the cervical spine and the foot.

Methods
Patients underwent either (1) sagittal T1-weighted or T2-weighted turbo spin-echo MRI of the cervical spine or (2) sagittal T1-weighted or proton density-weighted MRI of the foot including acquisitions without fat saturation, with $CHESS_{standard}$, with $CHESS_{SPSP}$, and with Dixon imaging (in-phase and water-only reconstructions). Signal suppression ratios (SSRs) were determined from regions of interest (ROI) placed in the subcutaneous fat of the neck as well as the proximal phalanges and metatarsal heads of the foot. Coefficients of variation (CoVs) were calculated from signal intensity measurements in the vertebral bodies of C3, C7, and T4 and across the metatarsophalangeal joints 1–5. Three readers ranked the images individually regarding the overall diagnostic quality. The Friedman test with post hoc Wilcoxon signed-rank tests was used for all group comparisons. Kendall's W was calculated for inter-reader agreement. Holm correction was applied to account for multiple testing.

Results
Thirty patients underwent cervical spine MRI, and 31 patients underwent foot MRI. In the cervical spine, SSR was 51% (± 17%), 89% (± 5%), and 88% (± 6%) for $CHESS_{standard}$, $CHESS_{SPSP}$, and Dixon, respectively, with significant differences between techniques ($p < 0.05$). In the foot, the mean SSR was 63% (± 16%), 85% (± 6%), and 87% (± 3%). Signal intensity CoV was highest for $CHESS_{standard}$ and lowest for Dixon in both body regions. Qualitative ratings preferred Dixon and $CHESS_{SPSP}$ over $CHESS_{standard}$ for cervical spine MRI, whereas $CHESS_{SPSP}$ was rated higher than Dixon and $CHESS_{standard}$ for foot MRI.

Conclusion
$CHESS_{SPSP}$ significantly improved fat saturation and signal homogeneity compared to $CHESS_{standard}$ in both the cervical spine and the foot. In both regions, radiologists preferred $CHESS_{SPSP}$ over $CHESS_{standard}$.

Introduction

Differentiating between fat and other high-signal tissues on MRI requires reliable fat suppression. Conventional fat saturation utilizes the slight difference in resonance frequency between protons in fat and water, known as the chemical shift. In theory, a radiofrequency (RF) pulse tuned to the fat-specific frequency and followed by a spoiler gradient suppresses the fat signal in the following acquisition. This chemical shift-selective fat saturation approach ($CHESS_{standard}$) frequently fails in the presence of inhomogeneities of the static magnetic field (B_0) and subsequently altered resonance frequencies [1, 2].

The Dixon technique is based on the same physical principle, but leverages the relative phase evolution of fat and water protons. In Dixon imaging, fat suppression is achieved by acquiring two images, an in-phase and an opposed-phase image, which allow the calculation of a water-only image. However, conventional Dixon imaging increases the acquisition time due to multiple acquisitions

[3–5]. Modern fast Dixon implementations acquire multiple echoes within a single echo train, but may show reduced SNR [6–8].

Recently, spectral-spatial RF pulses ($CHESS_{SPSP}$) have been proposed to improve CHESS. These RF pulses can be individually adjusted to local B_0 inhomogeneities based on previous B_0-mapping and subsequent pulse optimization [2].

We hypothesize that $CHESS_{SPSP}$ increases signal suppression and signal homogeneity in MRI of the cervical spine and the foot compared with $CHESS_{standard}$. In addition, we investigate whether radiologists prefer $CHESS_{SPSP}$ over $CHESS_{standard}$.

Methods

Study design

A prospective trial was conducted at University Medical Center Göttingen after approval by the institutional review board.

Cervical spine patients underwent either contrast-enhanced T1-weighted (T1w) or unenhanced T2-weighted (T2w) sagittal MRI, which included a turbo spin-echo (TSE) protocol without fat saturation, a protocol using standard fat saturation ($CHESS_{standard}$), and a protocol using patient-specific spectral-spatial RF pulses. In addition, a TSE Dixon protocol was acquired as a reference for robust fat suppression. All parameters were kept consistent across the T1w and T2w protocols, except for the receiver bandwidth, which was increased from 190 Hz/px to 840 Hz/px and from 219 Hz/px to 496 Hz/px for T2w and T1w fast Dixon protocols, respectively, to enable rapid sampling and ensure acquisition times comparable to the other protocols.

Foot patients underwent contrast-enhanced sagittal T1 MRI or proton density-weighted (PD) MRI using the same sequence of protocols with and without fat suppression. Bandwidth was adjusted for Dixon protocols from 204 Hz/px to 359 Hz/px for PD and from 229 Hz/px to 386 Hz/px for T1 protocols.

MRI technique

An automatic patient-specific spectral-spatial pulse design technique ($CHESS_{SPSP}$) was implemented on our 1.5T MRI scanner (MAGNETOM Flow.Elite) as a "push-button" option (BioMatrix Shim, software version *syngo* MR XB20) based on the method proposed by Eisen et al. [2].

Optimization consisted of two steps: First, a B_0 map was acquired to measure local B_0 inhomogeneities of the static magnetic field of the scanned patient [9]. Based on this acquisition and a predefined gradient shape, a spectral-spatial RF pulse was optimized to reach a target flip angle of 110° for fat in the imaging plane. This usually time-consuming process was significantly accelerated through various simplifications as described by Eisen et al. [2]. This process required 22 seconds for the acquisition of the B_0 map and an additional 3–4 seconds for the pulse optimization. $CHESS_{standard}$, however, requires advanced shimming procedures, which also require an acquisition of a B_0-map and subsequent optimization of compensatory shim currents. In contrast, $CHESS_{SPSP}$ requires only a basic shim predetermined by the manufacturer, resulting in comparable acquisition times.

Measurement of fat signal suppression

Polygonal regions of interest (ROIs) were placed in the dorsal subcutaneous tissue in a central slice of the image stacks and matched anatomically across the different protocols. The same was done for ROIs in the metatarsophalangeal (MTP) joints, specifically in the base of the proximal phalanx and the metatarsal head. For every fat suppression technique, we determined the signal suppression ratio (SSR) from the measured signal intensities in fat suppressed (SI_{fs}) and non-fat suppressed images (SI_{nfs}) (Formula 1). For the Dixon technique, the SSR was calculated from the in-phase and water-only images.

Formula 1

$$SSR = \frac{SI_{nfs} - SI_{fs}}{SI_{nfs}} \times 100$$

Measurement of signal homogeneity

In the fat-suppressed images, polygonal ROIs were placed in the vertebral bodies of C3, C7, and T4 in a central slice. To assess signal homogeneity, coefficients of variation (CoVs) were calculated for each patient and technique as the standard deviation of signal intensity measurements across the three levels divided by their mean. This was repeated for signal intensity measurements across the MTP joints.

Assessment of image quality

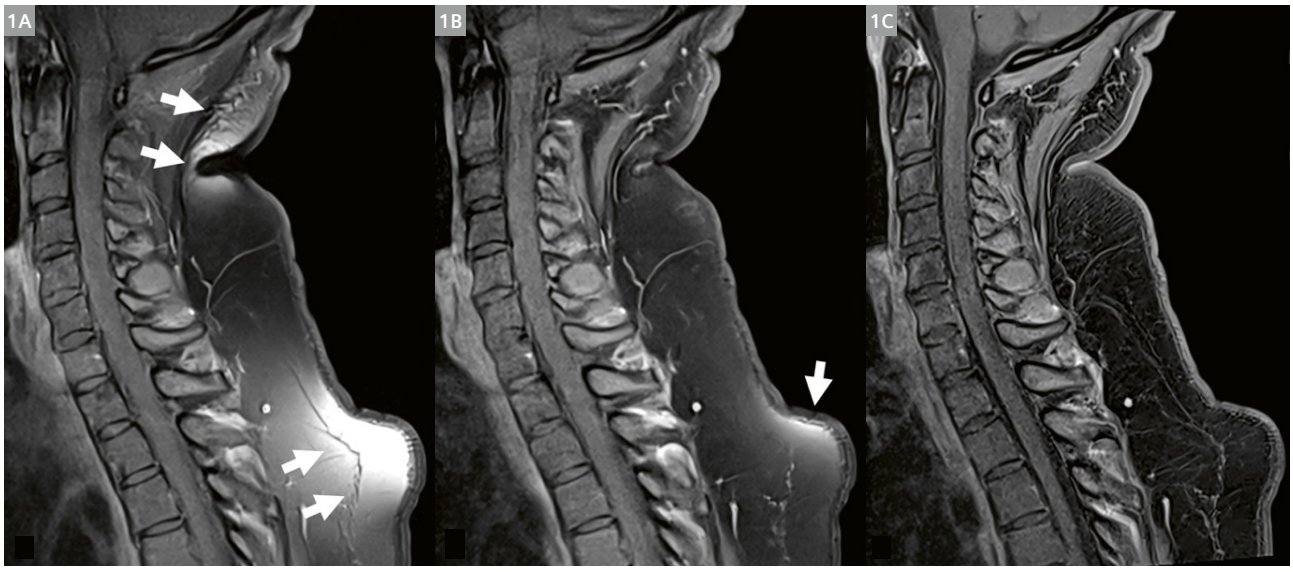
Three radiologists with 10, 6, and 2 years of experience independently ranked the techniques in each patient by assigning them a value between 1 (preferred) and 3 (worst). This was done for both foot MRI and cervical spine MRI.

Statistical analysis

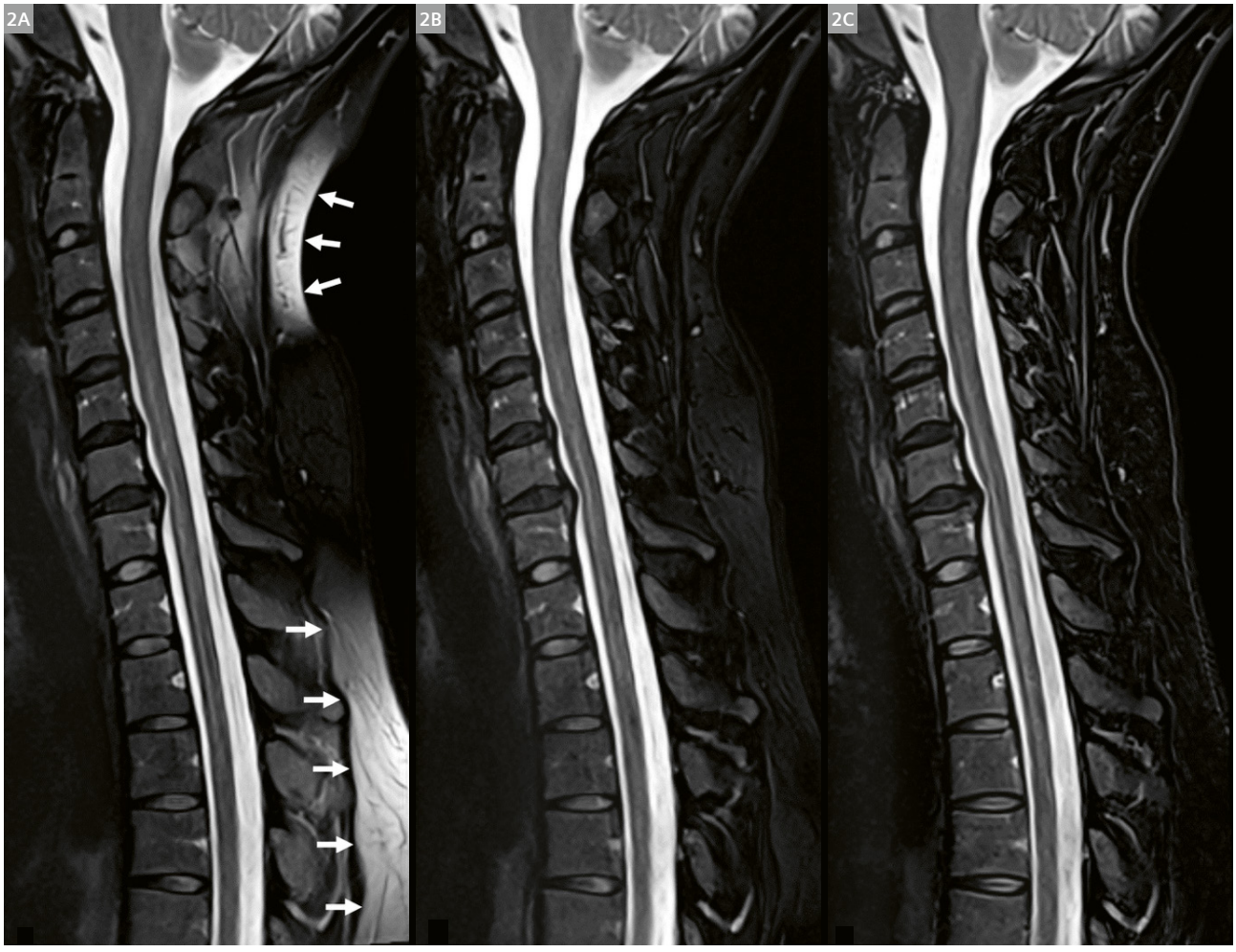
Descriptive statistics included mean and standard deviation for continuous variables, and median and interquartile ranges for ordinal variables.

Due to non-normality of the collected data, a non-parametric Friedman test was used for all group comparisons with post hoc Wilcoxon signed-rank tests performed pairwise.

Kendall's W with tie correction was used to determine rank agreement among readers. The level of significance was set at 0.05 for this study. Within each test family, *p*-values were adjusted for multiple testing using the Holm method.



1 Image panel showing sagittal, contrast-enhanced T1 TSE MRI of the cervical spine with **(1A)** $CHESS_{standard}$, **(1B)** $CHESS_{SPSP}$, and **(1C)** Dixon (water-only). White arrows indicate areas of failed fat suppression.



2 Image panel showing sagittal T2w TSE MRI of the cervical spine with **(2A)** $CHESS_{standard}$, **(2B)** $CHESS_{SPSP}$, and **(2C)** Dixon (water-only). White arrows indicate areas of failed fat suppression.

Results

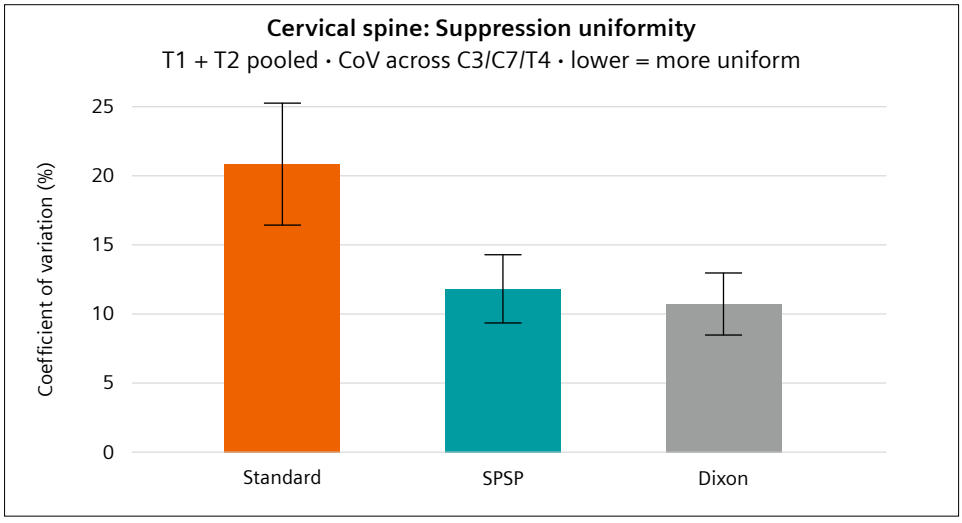
A total of 61 patients were included in this study, 30 of whom received cervical spine MRI (16 T1 MRI, 14 T2 MRI) and 31 received foot MRI (19 T1 MRI, 12 PD MRI).

Cervical spine MRI

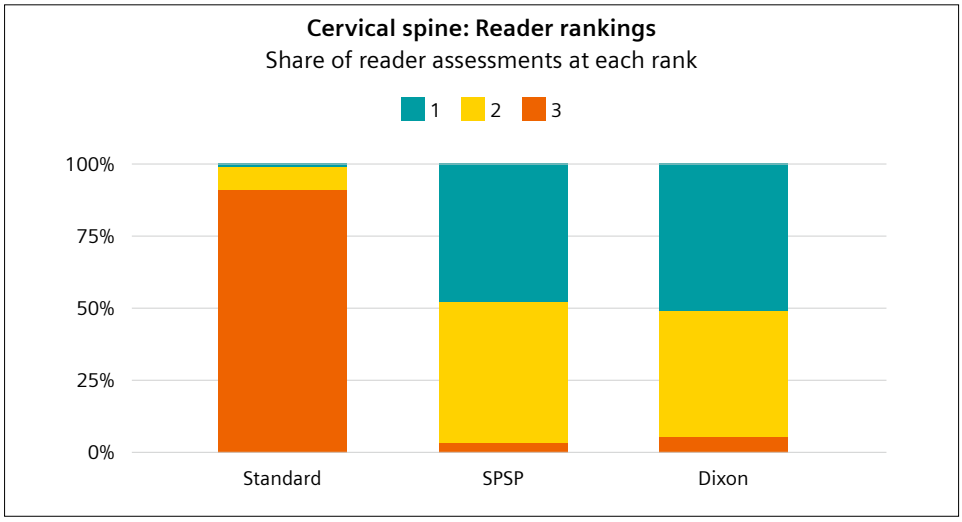
In the dorsal subcutaneous fat, the mean SSR was 51% (± 17%), 89% (± 5%), and 88% (± 6%) for $CHESS_{standard}$, $CHESS_{SPSP}$, and Dixon, respectively (Fig. 1 and Fig. 2). There was significant variation among the techniques (Friedman $\chi^2 = 46.07$, $p < 0.001$). Pairwise comparisons showed that SSR for Dixon and $CHESS_{SPSP}$ was significantly higher than for $CHESS_{standard}$ ($p < 0.001$). The difference between Dixon and $CHESS_{SPSP}$ did not reach significance ($p = 0.532$).

The CoV of signal intensity across the three spine levels was 21% (± 12%), 12% (± 7%), and 11% (± 6%) for $CHESS_{standard}$, $CHESS_{SPSP}$, and Dixon, respectively (Fig. 3). There were significant differences between techniques (Friedman $\chi^2 = 9.9$, $p < 0.007$), and pairwise comparisons demonstrated significantly higher signal uniformity for Dixon and $CHESS_{SPSP}$ than for $CHESS_{standard}$ ($p < 0.001$ and 0.003). Dixon and $CHESS_{SPSP}$ did not differ significantly regarding signal uniformity (Holm adj. $p = 0.579$).

Radiologist preference ratings showed very strong agreement (Kendall's W 0.89). Median ranks and interquartile ranges were 3 (IQR 0), 2 (IQR 1), and 1 (IQR 1) for $CHESS_{standard}$, $CHESS_{SPSP}$, and Dixon, respectively. There was significant variation among techniques (Friedman $\chi^2 = 109.4$, $p < 0.001$), and pairwise comparisons showed significantly higher ratings for Dixon and $CHESS_{SPSP}$ than for $CHESS_{standard}$ (both $p < 0.001$), whereas Dixon and $CHESS_{SPSP}$ did not differ significantly ($p = 0.932$). Figure 4 shows the share of ratings given to each technique, with similar distributions for Dixon and $CHESS_{SPSP}$.



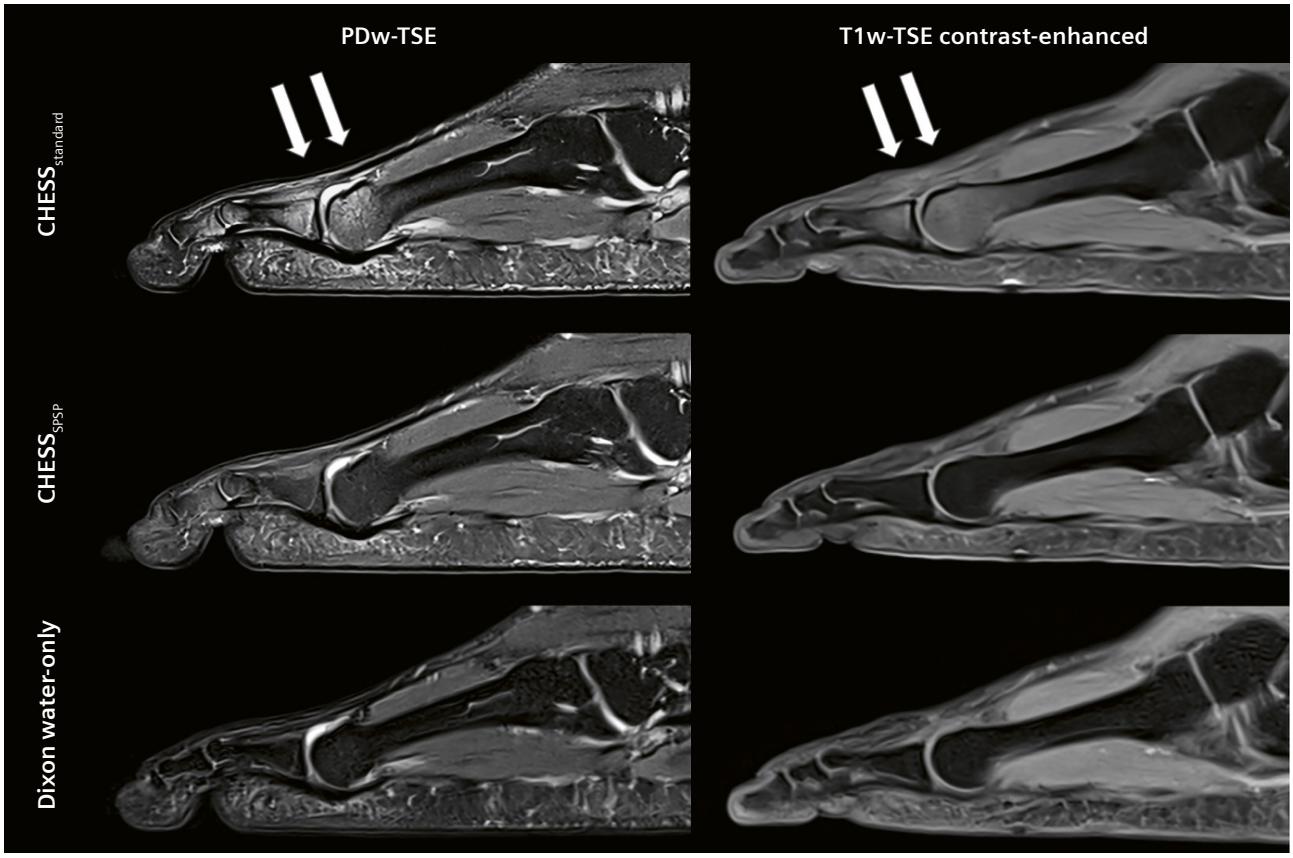
3 Spatial variation across spine levels C3/C7/T4. Error bars indicate 95% confidence intervals.



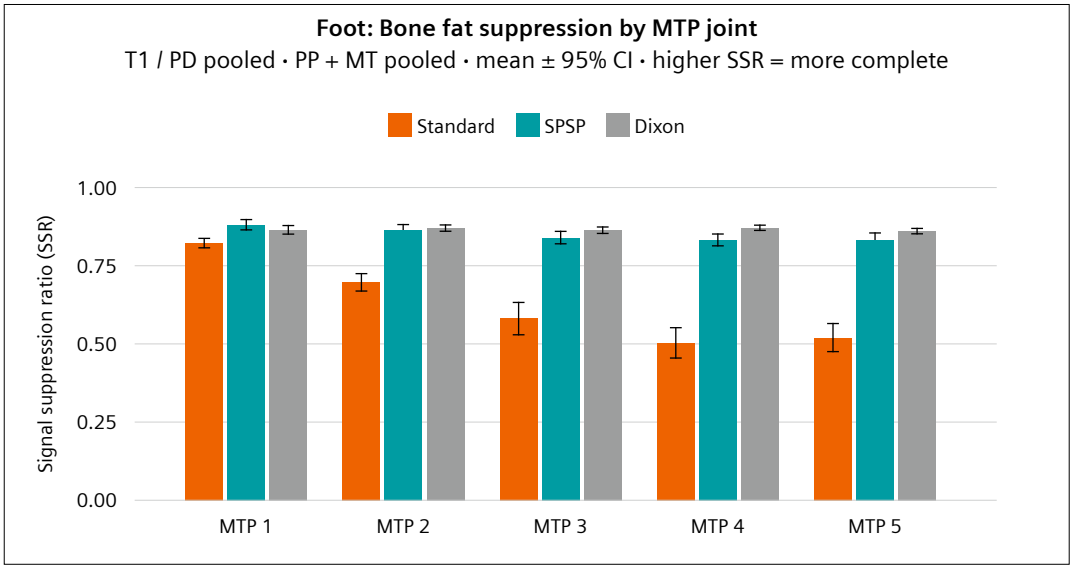
4 Distribution of reader rankings for each of the three techniques for cervical spine MRI.

Foot MRI

Across all MTP joints, the mean SSR in the proximal phalanges and metatarsal heads was 63% (± 16%), 85% (± 6%), and 87% (± 3%) (Fig. 5). Figure 6 shows the SSR distribution across the MTP joints. Mean SSR differed significantly across techniques (Friedman $\chi^2 = 54.5$, $p < 0.001$). $CHESS_{SPSP}$ and Dixon showed significantly higher SSR than $CHESS_{standard}$ ($p < 0.001$), and Dixon was superior to $CHESS_{SPSP}$ ($p = 0.026$).



5 Image panel showing sagittal PDw TSE and contrast-enhanced T1w TSE MRI of the forefoot for $CHESS_{standard}$, $CHESS_{SPSP}$, and Dixon water-only images. White arrows indicate areas of failed fat suppression.



6 Comparison of SSR in the three techniques across the five MTP joints.

The mean signal intensity CoV across the MTP joints was 24% (± 14%), 3% (± 2%), and 2% (± 1%) for $CHESS_{standard}$, $CHESS_{SPSP}$, and Dixon, respectively. Group differences were significant (Friedman $\chi^2 = 47.7$, $p < 0.001$), and pairwise comparisons showed superiority of Dixon over $CHESS_{SPSP}$ and $CHESS_{standard}$, whereas $CHESS_{SPSP}$ was superior to $CHESS_{standard}$ (all $p < 0.001$).

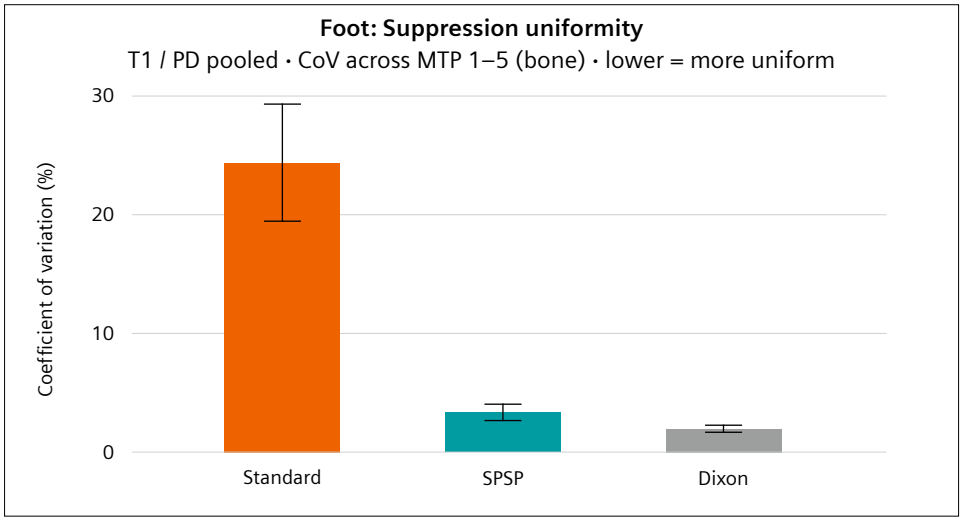
Radiologists' preference rankings showed very strong agreement (Kendall's W 0.77). They preferred $CHESS_{SPSP}$ (median rank 1, IQR 1) over Dixon (2, IQR 0), and $CHESS_{standard}$ (3, IQR 0) (Fig. 8). There were significant rank differences among all three techniques (Friedman $\chi^2 = 86.0$, $p < 0.001$) and in pairwise comparisons ($p < 0.001$).

Discussion

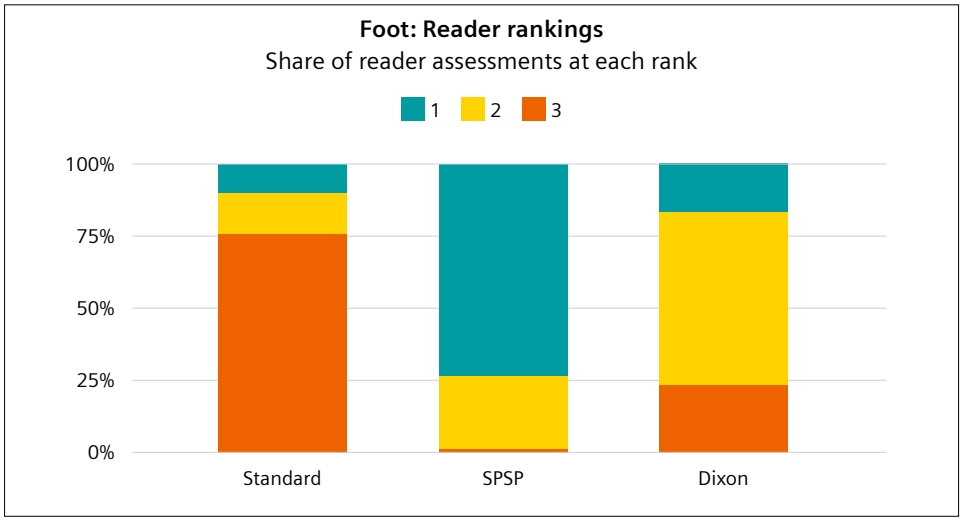
This study demonstrates a significant improvement in fat saturation with the clinical implementation of a patient-specific spectral-spatial pulse design. Compared to $CHESS_{standard}$, $CHESS_{SPSP}$ showed an absolute increase in signal reduction by 38 percentage points in the subcutaneous fat of the cervical spine, which corresponds to a relative improvement of 75%. In addition, $CHESS_{SPSP}$ demonstrated better signal homogeneity across multiple levels in the spine and was preferred by radiologists rating overall diagnostic image quality.

Several techniques have been proposed for spectral-spatial fat suppression [10, 11]. However, in vivo experiments are mostly limited by small study cohorts or time-consuming optimization procedures. The accelerated method proposed by Eisen et al., which served as the basis for this study, has made $CHESS_{SPSP}$ feasible for clinical use. In five healthy volunteers the reported signal reduction was 42% compared to $CHESS_{standard}$, which is consistent with our observations.

In the bone marrow of the foot, $CHESS_{SPSP}$ showed a 22-percentage-point increase in signal suppression compared to $CHESS_{standard}$, corresponding to a relative increase



7 Signal uniformity across the MTP joints for the three techniques.



8 Distribution of reader rankings for each of the three techniques for cervical spine MRI.

of 35%. $CHESS_{SPSP}$ demonstrated substantially improved signal uniformity, which did not reach the level of Dixon. In contrast to the cervical spine, radiologists agreed strongly in their overall preference for $CHESS_{SPSP}$ over Dixon and $CHESS_{standard}$. Although not quantified in this study, this may be explained by increased noise in fast Dixon acquisitions as a result of increased receiver bandwidth. As conventional Dixon methods require significantly longer acquisition times, this protocol choice was made to enable a comparison between three protocols with similar acquisition times.

In cervical spine MRI, signal suppression was slightly higher for $CHESS_{SPSP}$ than for Dixon. As Dixon represents the most robust fat suppression technique, we argue that this does not reflect superior fat suppression. In contrast to our results, Eisen et al. reported a higher signal reduction in fat for conventional Dixon than for $CHESS_{SPSP}$ [2]. Additionally, we observed that in a direct comparison between $CHESS_{SPSP}$ and $CHESS_{standard}$, slight differences in the signal intensity of the cerebrospinal fluid could be noted (Fig. 2). Although not quantified in this study, the cerebrospinal fluid appeared slightly darker on some images. Since a single pulse is used for all acquired slices, a possible explanation for these phenomena could be an inadvertent saturation of water affecting the signal intensity of the cerebrospinal fluid. As the subcutaneous region of interest does not exclusively contain fat, a higher signal suppression achieved by $CHESS_{SPSP}$ might reflect inadvertent water suppression in this compartment.

Conclusion

Fat saturation tends to fail in regions like the foot or the cervical spine, where susceptibility effects distort the static magnetic field. This study demonstrates that patient-specific spectral-spatial pulses ($CHESS_{SPSP}$) can recover much of this lost performance. $CHESS_{SPSP}$ significantly increased signal suppression in the subcutaneous fat of the cervical spine and the bones of the MTP joints by 75% and 35% compared to $CHESS_{standard}$. In addition, $CHESS_{SPSP}$ increased signal homogeneity across all five MTP joints and the vertebral bodies from C3 to T4. In terms of image quality, radiologists ranked $CHESS_{SPSP}$ higher than $CHESS_{standard}$ and considered it equivalent to Dixon for the cervical spine, whereas $CHESS_{SPSP}$ was preferred over Dixon for the foot. This matters for diagnostic accuracy in cases where failed fat suppression can mimic contrast enhancement or bone marrow edema.

$CHESS_{SPSP}$ can easily be added onto conventional TSE protocols, which preserves the familiar contrast behavior and high SNR. Although Dixon remains more robust in terms of signal uniformity, $CHESS_{SPSP}$ may become the preferred method in cervical spine patients with increased BMI or in peripheral regions like the foot.

Contact

Jonathan van Dieken, M.D.
Department of Clinical and
Interventional Radiology
University Medical Center Göttingen
Robert-Koch-Strasse 40
37075 Göttingen
Germany
jonathan.vandieken@med.uni-goettingen.de



References

1 Guerini H, Omoumi P, Guichoux F, Vuillemin V, Morvan G, Zins M, et al. Fat suppression with Dixon techniques in musculoskeletal magnetic resonance imaging: A pictorial review. Semin Musculoskelet Radiol [Internet]. 2015;19(4):335–47. Available from: http://dx.doi.org/10.1055/s-0035-1565913
2 Eisen CK, Liebig P, Herrler J, Ritter D, Lévy S, Uder M, et al. Fast online spectral-spatial pulse design for subject-specific fat saturation in cervical spine and foot imaging at 1.5 T. MAGMA [Internet]. 2024;37(2):257–72. Available from: http://dx.doi.org/10.1007/s10334-024-01149-8
3 Omoumi P. The Dixon method in musculoskeletal MRI: from fat-sensitive to fat-specific imaging. Skeletal Radiol [Internet]. 2022;51(7):1365–9. Available from: http://dx.doi.org/10.1007/s00256-021-03950-1
4 Dixon WT. Simple proton spectroscopic imaging. Radiology [Internet]. 1984;153(1):189–94. Available from: http://dx.doi.org/10.1148/radiology.153.1.6089263
5 Gaddikeri S, Mossa-Basha M, Andre JB, Hippe DS, Anzai Y. Optimal fat suppression in head and neck MRI: Comparison of multipoint Dixon with 2 different fat-suppression techniques, spectral presaturation and inversion recovery, and STIR. AJNR Am J Neuroradiol [Internet]. 2018;39(2):362–8. Available from: http://dx.doi.org/10.3174/ajnr.A5483
6 Date T, Redpath TW, Bussell DM. A bandwidth indicator for magnetic resonance imagers. Med Phys [Internet]. 1997;24(5):733–5. Available from: http://dx.doi.org/10.1118/1.597994
7 Son JB, Hwang KP, Madewell JE, Bayram E, Hazle JD, Low RN, et al. A flexible fast spin echo triple-echo Dixon technique: Flexible FTED. Magn Reson Med [Internet]. 2017;77(3):1049–57. Available from: http://dx.doi.org/10.1002/mrm.26186
8 Ma J, Son JB, Zhou Y, Le-Petross H, Choi H. Fast spin-echo triple-echo dixon (fTED) technique for efficient T2-weighted water and fat imaging. Magn Reson Med [Internet]. 2007;58(1):103–9. Available from: http://dx.doi.org/10.1002/mrm.21268
9 Majewski K. Simultaneous optimization of radio frequency and gradient waveforms with exact Hessians and slew rate constraints applied to kT-points excitation. J Magn Reson [Internet]. 2021;326:106941. Available from: http://dx.doi.org/10.1016/j.jmr.2021.106941
10 Shao X, Zhang Z, Zhong W, Guo H, Ugurbil K, Wu X. Comprehensive 4D parallel transmission spatial-spectral pulse design for slab-selective uniform water-selective excitation: Demonstration in the human brain at 7 Tesla. Magn Reson Med [Internet]. 2026;95(4):2052–62. Available from: http://dx.doi.org/10.1002/mrm.70183
11 Zhao F, Nielsen JF, Noll DC. Four dimensional spectral-spatial fat saturation pulse design. Magn Reson Med [Internet]. 2014;72(6):1637–47. Available from: http://dx.doi.org/10.1002/mrm.25076